Journal of
Applied Remote Sensing

Long-wave infrared imaging of vegetation for detecting leaking CO_2 gas

Jennifer E. Johnson
Joseph A. Shaw
Rick Lawrence
Paul W. Nugent
Laura M. Dobeck
Lee H. Spangler

Long-wave infrared imaging of vegetation for detecting leaking CO_2 gas

Jennifer E. Johnson,[a] Joseph A. Shaw,[a] Rick Lawrence,[b] Paul W. Nugent,[a] Laura M. Dobeck,[c] and Lee H. Spangler[d]

[a]Montana State University, Electrical and Computer Engineering Department, Bozeman, Montana 59717-3780
jshaw@ece.montana.edu

[b]Montana State University, Land Resources and Environmental Sciences Department, Bozeman, Montana 59717-3120

[c]Energy Research Institute, Montana State University, Bozeman, Montana 59717-2465

[d]Montana State University, Chemistry and Biochemistry Department, Bozeman, Montana 59717-3780

Abstract. The commercial development of uncooled-microbolometer, long-wave infrared (LWIR) imagers, combined with advanced radiometric calibration methods developed at Montana State University, has led to new uses of thermal imagery in remote sensing applications. One specific novel use of these calibrated imagers is imaging of vegetation for CO_2 gas leak detection. During a four-week period in the summer of 2011, a CO_2 leak was simulated in a test field run by the Zero Emissions Research and Technology Center in Bozeman, Montana. An LWIR imager was deployed on a scaffold before and during the CO_2 release, viewing a vegetation test area that included regions of high and low CO_2 flux. Increased root-level CO_2 concentration caused plant stress that led to reduced thermal regulation of the vegetation, which was consistent with increased diurnal variation of IR emission observed in this study. In a linear regression, the IR data were found to have a strong relationship to the CO_2 emission and to be consistent with the location of leaking CO_2 gas. Reducing the continuous data set to one image per day weakened the regression fit, but maintained sufficient significance to indicate that this method could be implemented with once-daily airborne images. [DOI: 10.1117/1.JRS.6.063612]

Keywords: remote sensing; infrared imaging; thermal imaging; vegetation sensing.

Paper 12283P received Sep. 13, 2012; revised manuscript received . NaN, ; accepted for publication Nov. 12, 2012; published online Dec. 10, 2012.

1 Introduction

The recent increase in availability and capabilities of ultra-compact, uncooled, microbolometer thermal imagers is enabling many new remote sensing applications. However, quantitatively demanding applications require very careful calibration. At Montana State University, we have developed novel methods for achieving and maintaining radiometric calibration for wide-angle, long-wave infrared (LWIR) microbolometer imagers, initially for measuring clouds in climate science and Earth-space optical communications.[1,2,3] These imagers are an order of magnitude smaller and cheaper, while also consuming less power than typical cooled IR imagers. Using the newly developed calibration methods allows the imagers to be calibrated in the laboratory and deployed in the field without an onboard calibration target, thereby making them ideal for a variety of new remote sensing purposes.

One such application is the IR imaging of vegetation to detect a CO_2 gas leak through an induced change in plant stress. This was demonstrated experimentally in a controlled gas release experiment conducted by the Zero Emissions Research and Technology (ZERT) Center in Bozeman, Montana. The field has been used from 2007 to 2012 for researching methods of detecting leaks at a geologic carbon sequestration facility. Technologies tested in these experiments

0091-3286/2012/$25.00 © 2012 SPIE

include optical spectroscopic detection of gas leakage[4] and hyperspectral and multispectral imaging to observe changes in the reflectance of vegetation exposed to elevated concentrations of CO_2 gas.[5–9] Here, we report on the use of LWIR imaging of vegetation to locate the leaking gas. The premise behind imaging the vegetation is that higher CO_2 concentrations in the soil will stress the vegetation, leading to measurable changes in long-wave emission. Higher gas concentrations in soil could result in less oxygen and water being drawn from the soil into the roots, causing the leaf stomata to close and changing the reflectance and emission properties of the vegetation. The mechanism that we expect will lead to changed LWIR emission is that the stressed vegetation experiences a reduced rate of transpiration,[10] causing an impaired ability to regulate its own temperature as the ambient air temperature changes during the day and night. During the summers of 2009, 2010, and 2011, we deployed a radiometrically calibrated LWIR microbolometer-based imager in the field to compare the radiance of exposed vegetation with that of healthy vegetation, thereby identifying CO_2 gas leak locations.

Thermal imaging of vegetation has been used numerous times in various studies. Satellite and airborne thermal IR imagers have been used to both classify terrain vegetation[11] and determine surface soil water content.[12,13] These studies relate the satellite-derived surface radiant temperature of the vegetation to the normalized difference vegetation index (NDVI) determined from satellite visible and near-IR data. Airborne systems have also used thermal IR multispectral scanners to measure the thermal energy responses of vegetation for examining the thermal dynamics of urban vegetation.[14] Ground-level IR imagers have been used to determine the leaf-canopy temperatures of vegetation for predicting high leaf water potential.[15,16] Our research expands on these previous efforts to investigate the effect of CO_2-induced stress on the thermal responses of vegetation.

2 Methodology

The ZERT field is a hayfield located just west of the Montana State University campus in Bozeman, Montana. A horizontal well was buried at a nominal depth of 2 m and divided into six segments. Approximately 0.55% of the pipe was open to allow the CO_2 gas to escape.[4] The gas release periods were July 15 to August 12 in 2009, July 19 to August 15 in 2010, and July 15 to August 15 in 2011. The flow rate of the CO_2 through the well varied for each year of the release: 0.2 tons/day in 2009, 0.15 tons/day in 2010, and 0.15 tons/day in 2011.[8,9] Released CO_2 exited the ground with a highly nonuniform distribution, creating localized regions of elevated CO_2 concentrations that we refer to as hot spots.

Within the ZERT field, a vegetation patch of approximately 400 m^2 was the focus of the imaging experiments during the releases. The well ran along a single edge of the vegetation patch. We deployed vegetation imagers on a 3-m-tall scaffold located at the edge of the vegetation patch containing the well, as shown in Fig. 1. Images were acquired every 10 minutes throughout each day for the 2009 CO_2 release, every 5 minutes in 2010, and every 1 minute in 2011.

We used a FLIR Systems Inc. photon 320 camera to acquire thermal images at a nominally 45° viewing angle. The well ran horizontally though the bottom of the images, and a hot-spot region was located just to the right of the imaged area. Fig. 2 shows a wide-angle view of the vegetation test area seen from the top of the scaffold in the midst of the gas release experiment, with a white line denoting the approximate location of the underground horizontal well. The hot spot was at this time becoming visible to the eye, just below the white camera housing at the lower center portion of the image; however, the thermal images detected changes in the vegetation near this hot spot well before the changes were visually obvious. We did not directly image the center of the hot spot because vegetation there degraded rapidly during the release experiment; rather, we used image pixels near the edge of the hot spot as a test region and pixels far from the hot spot as control regions.

The images were radiometrically calibrated to radiance [$W/(m^2\,sr)$] using techniques developed at Montana State University, which rely on full characterization of the camera with a large-area blackbody source operated with the camera inside a thermal chamber to calibrate the imager at multiple operating temperatures.[17] Custom MATLAB software (MathWorks, Natick, Massachusetts) was used to select regions of interest in the images. Images acquired in 2009 and 2010 used a test region adjacent to the CO_2 hot spot and a single control region at the upper-left edge

Fig. 1 Scaffold used to mount the thermal IR imager (in the white tube) and a visible-near-infrared multispectral imager (in the white box with the open back).

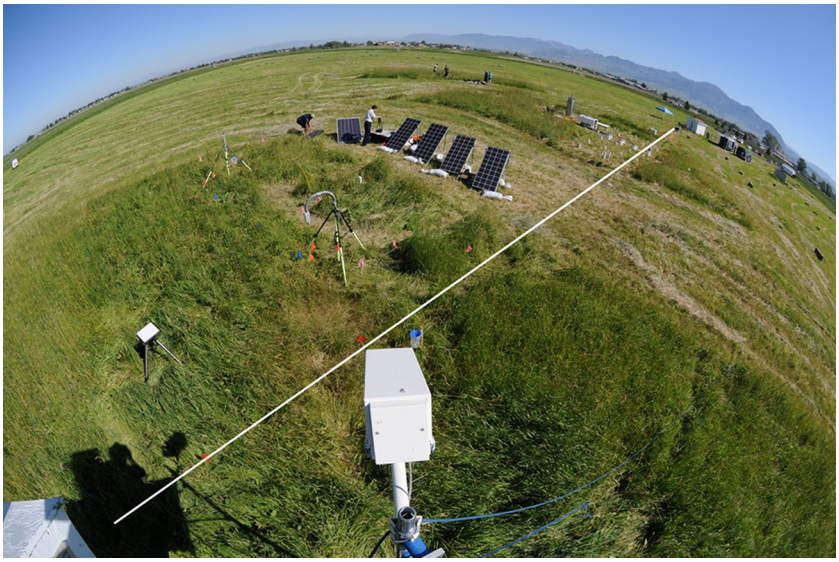

Fig. 2 Wide-angle view of the vegetation test area (lower left) at the ZERT field in Bozeman, Montana, with the white line indicating the approximate location of the underground well from which CO_2 gas was released.

of the vegetation images, where the CO_2 flux is generally near the background level. For the 2011 data, two control regions were chosen, which we refer to as a horizontal control region and a vertical control region (owing to their locations relative to the hot spot), along with the hot-spot region. Fig. 3 shows the location of the two control regions and the hot-spot region used to generate the statistical radiance values for the 2011 images.

We chose to use two control regions to investigate concerns over the camera viewing angle. Since the thermal IR imager viewed such a large area of vegetation from relatively close to the surface, the viewing angle changed notably between the bottom and top of the images. Using a control region in the same horizontal line as the hot-spot region, in addition to the control region

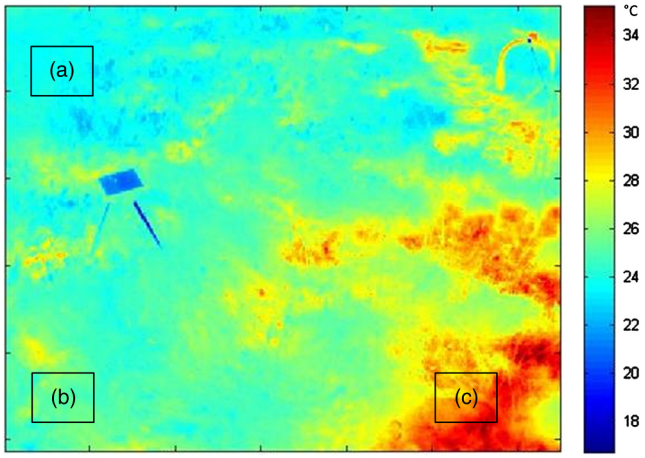

Fig. 3 Sample thermal IR image of the vegetation patch showing the regions of interest for the 2011 release: (a) the vertical control region, (b) the horizontal control region, and (c) the hot-spot region.

located diagonally from the hot spot, allowed this concern to be addressed by comparing any differences in the radiance emitted from both control regions. For each acquired image, we calculated spatial and temporal statistics of the radiance values as follows: the maximum and minimum differences between each region temperature and the ambient air temperature, the maximum and minimum temperature differences between the horizontal control region and the hot-spot region, and the maximum and minimum temperature differences between the vertical control region and the hot-spot region. Linear regressions were calculated, using experiment day as the response variable and the radiance statistics as predictors.

3 Results

Early images acquired during the 2009 release led us to believe that the high concentrations of CO_2 in the soil had a substantial effect on the LWIR emission from the vegetation. Our comparison of the diurnal trends, or daily brightness temperature time-series plots, from before and after the release shows a divergence of the hot-spot vegetation from the control region vegetation. Examples of these diurnal plots are shown in Fig. 4(a) for July 11, 2009, before the start of the release, and in Fig. 4(b) for August 26, 2009, after the end of the CO_2 release.

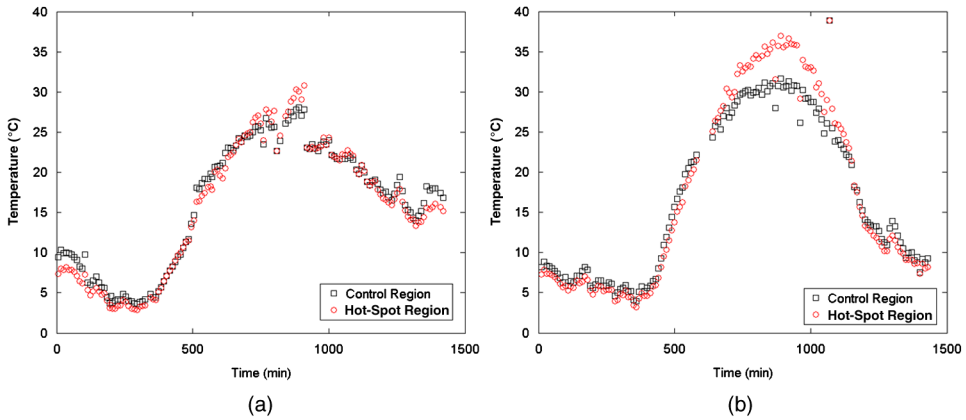

Fig. 4 Diurnal variation of the vegetation brightness temperature for (a) July 11, 2009, before the start of the CO_2 release and (b) August 26, 2009, after the end of the CO_2 release (the horizontal axes show a 24-hour period, plotted from midnight to midnight).

These plots show that the vegetation initially cooled off during the night and then gradually warmed up due to solar heating during the daytime. The vegetation reached a maximum temperature in the afternoon, at which point it began cooling off with lower solar elevation angles in the late afternoon. Before the start of the release, both the control region and the hot-spot region behaved nearly identically. However, this changed by the end of the gas release experiment, as shown in Fig. 4(b). The same solar heating trends were observed in the diurnal plots from before and after the CO_2 release; however, there was a notable difference between the control region and the hot-spot region during the warmest portion of the day by the end of the release [Fig. 4(b)]. This provided evidence that the higher concentration of CO_2 in the soil at the hot-spot region was affecting the vegetation and impairing the vegetation's ability to regulate its temperature.

Motivated by the intriguing patterns observed in the 2009 diurnal data, we conducted extended deployments of the thermal imager at the vegetation test field during gas releases in the summers of 2010 and 2011. Here, we show the results from the 2011 deployment, which again showed a difference in diurnal trends between the two control regions and the hot-spot region. Figure 5 shows that this difference was also readily observable in thermal images acquired before and after the release.

The vegetation nearest to the hot-spot region showed markedly higher temperatures than the vegetation that was unexposed to leaking CO_2. Figure 6 shows time-series plots of (a) the maximum temperature difference between the three regions and the ambient air

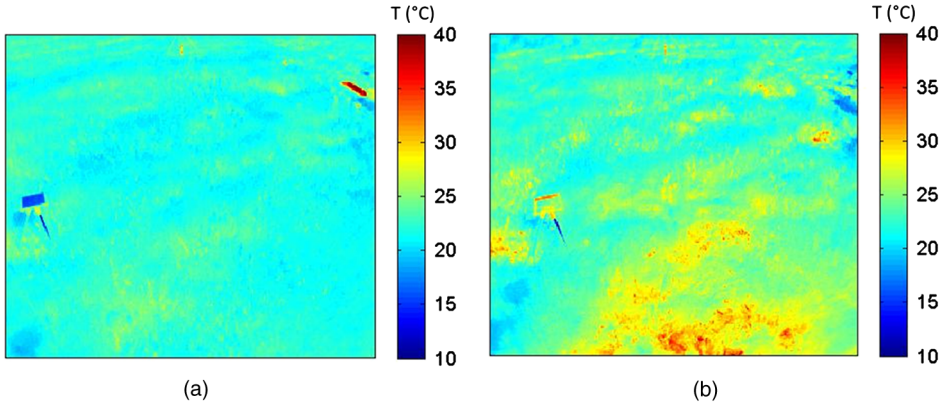

Fig. 5 LWIR images acquired at 10 a.m. (Mountain Daylight Time) on July 13, 2011 (a) and August 10, 2011 (b).

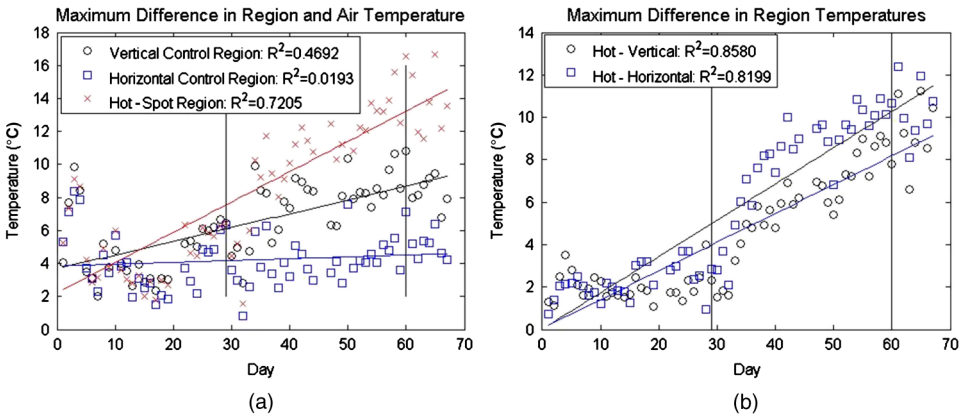

Fig. 6 Maximum temperature differences plotted versus day of the 2011 release, with the vertical lines representing the start and end of the gas release: (a) temperature difference between each vegetation region and the ambient air temperature, (b) temperature difference between the hot spot and each control region.

temperature, and (b) the maximum temperature difference between the two control regions and the hot-spot region. These two plots were found to yield the strongest coefficients of determination (R^2 values). Both control regions behaved similarly, while the hot-spot region was distinguishable from both of them. The temporal change of temperature near the hot spot consistently had a steeper slope than the change in either of the control regions. The similarity between the regression lines for the two control regions indicated that there was no major concern over the camera viewing angle.

The time-series plot of region differences in Fig. 6(b) is of particular interest since it shows a distinct change in the hot-spot brightness temperature almost immediately after the start of the CO_2 release. Conversely, plots showing the minimum difference in region and air temperature each day and the minimum difference in region temperatures each day gave extremely low R^2 values and provided very little useful information. The regression for the minimum difference in region and air temperature resulted in the following R^2 values: 0.112 (vertical control region), 0.066 (horizontal control region), and 0.090 (hot-spot region). The minimum region difference regression resulted in the following R^2 values: 0.003 (vertical control region) and 0.003 (horizontal control region).

We also found that it is possible to use images acquired during shorter time periods instead of relying on continual 24-hour time series. When we limited the data to the midday hours of 10 a.m. to 2 p.m., the R^2 values changed modestly. For the maximum difference of region and air temperatures, similar to Fig. 6(a), we found $R^2 = 0.288$ at the vertical control, 0.006 at the horizontal control, and 0.691 at the hot spot. For the maximum difference of region temperatures, similar to Fig. 6(b), we found $R^2 = 0.800$ for hot–spot vertical and 0.796 for hot–spot horizontal.

To explore the possibility of using thermal imaging for monitoring large areas or pipelines, perhaps from airborne platforms, we repeated the regressions using data from 1 p.m. and 3 a.m., near the maximum and minimum temperature extremes of each day. In this case, the R^2 values reduced to 0.163 for the vertical control and 0.497 for the hot spot, while increasing slightly to 0.272 for the horizontal control. Similar to Fig. 6(a), the hot-spot region still exhibited a steeper slope and a higher R^2 value than both control regions.

The ultimate simplification of the method was to use only one image from a fixed time each day. We selected 1 p.m. as our image time, since that was near the warmest time of the day when we typically observed the largest brightness temperature difference for healthy and stressed vegetation [Fig. 4(b)]. The results are plotted in Fig. 7 as the difference between each region's temperature and the ambient air temperature. The hot spot and control slopes and offsets were found to differ with statistical significance, although in this case there was a slight significance for the difference between the two control regression line slopes. Still, the analysis suggests that it is possible to obtain a statistically significant result from only one

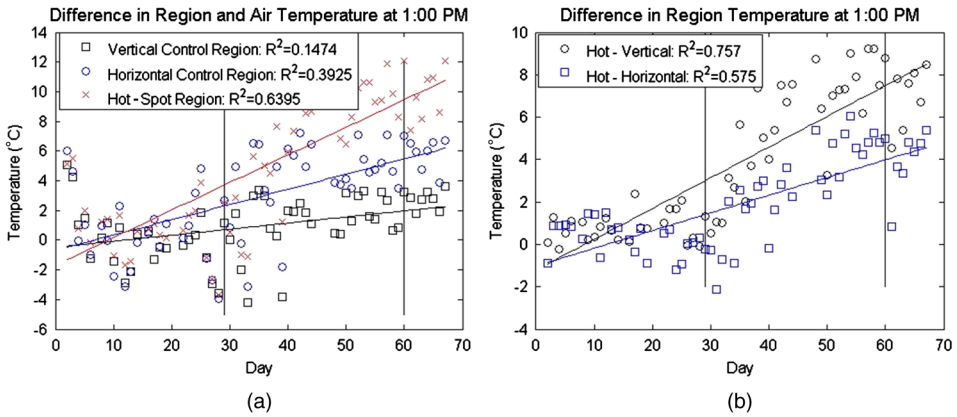

Fig. 7 Temperature differences at 1 p.m. between (a) regions and ambient air temperature, and (b) hot spot and the two control regions, plotted versus day. The vertical lines represent the start and end of the release.

image at a fixed time each day. In any of these methods, the thermal images would be used to locate regions to undergo further testing, and final confirmation of a leak would be made using *in situ* sensors.

4 Conclusion

Radiometrically calibrated microbolometer-based thermal imagers can substantially simplify the monitoring of carbon sequestration sites. They require no calibration target at the site, making imaging easy and practical. Our experiments showed that plant stress is evident in thermal imagery obtained from radiometrically calibrated imagers, allowing detection of vegetation affected by elevated levels of CO_2. Statistically, the thermal images showed a significant difference between the healthy vegetation and the exposed vegetation. This difference began almost immediately after the start of the CO_2 release and lasted throughout the test, indicating that it was not an artifact of coincidental environmental changes. The rapid change of exposed vegetation within a few days of the start of the CO_2 release showed that the thermal images are sensitive to vegetation changes induced by elevated ground-level gas concentrations. In all the maximum temperature difference plots, the hot-spot region was distinguishable from both control regions. While there was a slight difference between the two control regions, the difference was small enough to indicate that there was no major concern with the camera viewing angle. A method that relied on a single image instead of continuous imaging was explored and found to provide a sufficiently strong coefficient of determination for the hot spot. Since the hot spot is noticeably different from either control region, this method proves useful for distinguishing among locations with and without CO_2 leaks in a large monitoring area, thereby enabling the use of airborne thermal imaging.

Acknowledgments

This material is based upon work supported by the Department of Energy under award number DE-FE0000397. This report was prepared as an account of work sponsored by an agency of the U.S. government. Neither the U.S. government nor any agency thereof, nor any of their employees, makes any warranty, express or implied, or assumes any legal liability or responsibility for the accuracy, completeness, or usefulness of any information, apparatus, product, or process disclosed, or represents that its use would not infringe privately owned rights. Reference herein to any specific commercial product, process, or service by trade name, trademark, manufacturer, or otherwise does not necessarily constitute or imply its endorsement, recommendation, or favoring by the U.S. government or any agency thereof. The views and opinions of authors expressed herein do not necessarily state or reflect those of the U.S. government or any agency thereof.

References

1. J. A. Shaw et al., "Radiometric cloud imaging with an uncooled microbolometer thermal infrared camera," *Opt. Exp.* **13**(15), 5807–5817 (2005), http://dx.doi.org/10.1364/OPEX.13.005807.
2. B. Thurairaijah and J. A. Shaw, "Cloud statistics measured with the infrared cloud imager," *IEEE Trans. Geosci. Rem. Sens.* **43**(9), 2000–2007 (2005), http://dx.doi.org/10.1109/TGRS.2005.853716.
3. P. W. Nugent, J. A. Shaw, and S. Piazzolla, "Infrared cloud imaging in support of Earth-space optical communication," *Opt. Exp.* **17**(10), 7862–7872 (2009), http://dx.doi.org/10.1364/OE.17.007862.
4. L. H. Spangler et al., "A shallow subsurface controlled release facility in Bozeman, Montana, USA, for testing near surface CO_2 detection techniques and transport models," *Env. Earth Sci.* **60**(2), 227–239 (2010), http://dx.doi.org/10.1007/s12665-009-0400-2.

5. E. J. Male et al., "Using hyperspectral plant signatures for CO_2 leak detection during the 2008 ZERT CO_2 sequestration field experiment in Bozeman, Montana," *Env. Earth Sci.* **60**(2), 251–261 (2010), http://dx.doi.org/10.1007/s12665-009-0372-2.
6. G. J. Bellante, "Hyperspectral remote sensing as a monitoring tool for geological carbon sequestration," M.S. Thesis, Montana State University, Bozeman, http://etd.lib.montana.edu/etd/view/item.php?id=1440 (2011).
7. J. H. Rouse et al., "Multi-spectral imaging of vegetation for detecting CO_2 leaking from underground," *Env. Earth Sci.* **60**(2), 313–323 (2010), http://dx.doi.org/10.1007/s12665-010-0483-9.
8. J. A. Hogan et al., "Low-cost multispectral vegetation imaging system for detecting leaking CO_2 gas," *Appl. Opt.* **51**(4), 59–66 (2012), http://dx.doi.org/10.1364/AO.51.000A59.
9. J. A. Hogan et al., "Detection of leaking CO_2 gas with vegetation reflectance measured by a low-cost multispectral imager," *IEEE J. Selected Topics Appl. Earth Obs. Remote Sens.* **5**(3), 699–706 (2012), http://dx.doi.org/10.1109/JSTARS.2012.2202880.
10. H. G. Jones and E. Rotenberg, "Energy, radiation, and temperature regulation in plants," in *Encyclopedia of Life Sciences*, Wiley (2001).
11. C. P. Lo, D. A. Quattrochi, and J. C. Luvall, "Application of high-resolution thermal infrared remote sensing and GIS to assess the urban heat island effect," *Int. J. Remote Sens.* **18**(2), 287–304 (1997), http://dx.doi.org/10.1080/014311697219079.
12. R. R. Gillies and T. N. Carlson, "Thermal remote sensing of surface soil water content with partial vegetation cover for incorporation into climate models," *J. Appl. Meteorol.* **34**(4), 745–756 (1995), http://dx.doi.org/10.1175/1520-0450(1995)034<0745:TRSOSS>2.0.CO;2.
13. I. Sandholt, K. Rasmussen, and J. Andersen, "A simple interpretation of the surface temperature/vegetation index space for assessment of surface moisture status," *Remote Sens. Environ.* **79**(2–3), 213–224 (2002), http://dx.doi.org/10.1016/S0034-4257(01)00274-7.
14. D. A. Quattrochi, "Analysis of vegetation within a semi-arid urban environment using high spatial resolution airborne thermal infrared remote sensing data," *Atmos. Environ.* **32**(1), 19–33 (1998), http://dx.doi.org/10.1016/S1352-2310(97)00179-9.
15. A. Blum, J. Mayer, and G. Gozlan, "Infrared thermal sensing of plant canopies as a screening technique for dehydration avoidance in wheat," *Field Crop. Res.* **5**, 137–146 (1982), http://dx.doi.org/10.1016/0378-4290(82)90014-4.
16. I. Leinonen and H. G. Jones, "Combining thermal and visible imagery for estimating canopy temperature and identifying plant stress," *J. Exp. Bot.* **55**(401), 1423–1431 (2004), http://dx.doi.org/10.1093/jxb/erh146.
17. P. W. Nugent, J. A. Shaw, and N. J. Pust, "Correcting for focal plane array temperature dependence in microbolometer infrared cameras lacking thermal stabilization," *Opt. Eng.* **52**(6), in press (2013)

Jennifer Johnson received a bachelor's degree in mechanical engineering from Montana State University in 2009. She then got a master's degree in electrical engineering from Montana State University in 2012. The focus of her research was remote sensing applications of uncooled LWIR imagers.

Joseph A. Shaw is the director of the Optical Technology Center, a professor of electrical and computer engineering, and an affiliate professor of physics at Montana State University in Bozeman, Montana. He received PhD and MS degrees in optical sciences from the University of Arizona, an M.S. degree in electrical engineering from the University of Utah, and a BS degree in electrical engineering from the University of Alaska–Fairbanks. He is a fellow of the Optical Society of America and SPIE. He conducts research on the development and application of radiometric, polarimetric, and laser-based optical remote sensing systems.

Rick Lawrence is a professor of remote sensing at Montana State University and director of its Spatial Sciences Center. He received his B.A. in political science from Claremont McKenna College, a J.D. from Columbia University, and an M.S. and Ph.D in forest resources from Oregon State University.

Paul W. Nugent is a research engineer with the Electrical and Computer Engineering Department at Montana State University and president of NWB Sensors Inc., in Bozeman, Montana. He received his M.S. and B.S. degrees in electrical engineering from Montana State University. His research activities include radiometric thermal imaging and optical remote sensing.

Laura M. Dobeck received a B.S. degree in chemistry from the University of Wisconsin–Madison in 1991, and M.S. and Ph.D degrees in physical chemistry from Cornell University in Ithaca, New York, in 1994 and 1999, respectively. She has studied reaction dynamics of small molecules in the gas phase using laser spectroscopy and electron transfer in the solution phase with ultrafast laser systems. Her current interests include studying the transport of CO_2 in the near-ground surface and testing and evaluating surface and near-subsurface monitoring techniques to be applied to geological carbon dioxide sequestration. She currently serves as the field site manager for the ZERT shallow subsurface CO_2 controlled release facility at Montana State University in Bozeman. She is a member of the American Geophysical Union.

Lee H. Spangler received a B.A. degree at Washington & Jefferson College in 1980 and a Ph.D in physical chemistry at the University of Pittsburgh in 1985. He was a postdoctoral researcher at Los Alamos National Laboratory in New Mexico from 1985 to 1987. He joined the chemistry faculty at Montana State University in 1987, where he now serves as the director of the Energy Research Institute and associate vice president for research.